ELSEVIER

International Journal of Heat and Fluid Flow 20 (1999) 395–401

International Journal of HEAT AND FLUID FLOW

www.elsevier.com/locate/ijhff

Investigations on inward flow between two stationary parallel disks

A. Singh [a,*], B.D. Vyas [b,1], U.S. Powle [b]

[a] Newgen Software Technologies Ltd., A-6 Satsang Vihar Marg, Qutab Institutional Area, New Delhi 110067, India
[b] Indian Institute of Technology, Powai, Mumbai 400076, India

Received 20 February 1998; accepted 1 December 1998

Abstract

The present study examines the effect of acceleration on flow field. Both experimental and numerical methods have been employed to study the problem. Fluid enters through the peripheral gap between two concentric disks and converges to the center where it discharges axially through a hole in one of the disks. The mean flow governing equations have been solved in the numerical study. A low Reynolds number k–ε model has been used to model the Reynolds stresses. The experimental study involves the measurement of velocity field and turbulence intensity with laser Doppler anemometery. Both the studies show the change in flow regime from turbulent to laminar. The numerical study reveals that the acceleration parameter is not the only factor governing turbulent–laminar transition in this flow, the gap ratio also plays a significant role.

Keywords: Axisymmetric; Turbulence modelling; Stationary disks; Inward flow; Reverse transition

Notation

d	diameter of the disks
f	friction factor
G	gap ratio, h/r_2
h	half spacing between the disks
k	turbulence kinetic energy
$\bar{k}$	k/U^2
K_v	acceleration parameter
p	static pressure
$\bar{p}$	$p/(\rho U_2^2)$
Q	flow rate
r	radial coordinate
$\bar{r}$	r/r_2
Re_l	$4Uh/v$, local Reynolds number
u	radial velocity
$\bar{u}$	u/U
u_τ	$[v\ \{\partial u/\partial z\}_{z=0}]^{1/2}$
u^+	u/u_τ
U	$Q/(4\pi hr)$
U_∞	free stream velocity
w	axial velocity
z	axial coordinate
$\bar{z}$	z/h
z^+	$u_\tau z/v$
ε	dissipation rate
v	kinematic viscosity
v_t	turbulence viscosity
ρ	density

Superscript

$'$	fluctuating components

Subscript

1,2	quantities at inlet and exit, respectively

1. Introduction

The flow between two disks is a topic of much interest. The problem has attracted the attention of mathematicians and engineers alike. The problem allows the similarity solution with a potential of multiplicity of the solution, a matter of great interest to theoreticians. The inward flow resembles flows that occur in many engineering applications such as face seals, exit of a geothermal reservoir and disk type heat exchangers. Hence, it is equally important for engineers.

The inward laminar flow between two disks has been studied by many investigators. McGinn (1956) developed an expression for pressure distribution using the argument that the pressure variation is partly due to the inertial contribution and partly due to viscous dissipation. An experimental study on the unsteady air flow between two disks was carried out by Garcia (Garcia, 1969–1970). The measurements of velocity fluctuations using a constant temperature hot wire anemometer revealed that the amplitudes of oscillations were higher than the relevant value of turbulence fluctuations. Hence, the author concluded that the flow was inherently unstable. Murphy et al. (1978) studied the problem numerically. They found three regions; a region of strong viscous effects, a region of equal viscous and inertial effects and a region of strong inertial effects. The boundary layer was that of internal flow type in the first two regions, whereas it was an external flow

* Corresponding author.
[1] Late Professor.

0142-727X/99/$ – see front matter
PII: S0142-727X(98)10058-9

type in the third region. Using various definitions of acceleration parameters, they predicted different criteria of lower critical Reynold's numbers. An experimental study was carried out by Murphy et al. (1983) for laminar converging flow. The flow visualization and pressure distribution indicated that the change of flow regime might take place at a Reynolds number of 20,700. Lee and Lin (1985) derived an expression for radial pressure distribution. The closed form solutions for the prediction of radial pressure were derived by Vatistas (1988, 1990). The predictions of these closed form solutions were found to be in close agreement with experimental data.

The inward flow between two stationary disks is an accelerated flow. It has been found that the initially turbulent flow becomes laminar if subjected to an acceleration. This phenomenon has been discovered by measurements in accelerating flows by many investigators (Launder, 1964; Moretti and Kays, 1965). The change from turbulent to laminar flow has been reported by many investigators (Moller, 1963; Kreith, 1965; Tabatabai and Pollard, 1987; Ervin et al., 1989) for outward flow between two disks, a decelerating flow, even though the natures of accelerating and decelerating flows are opposite to each other. The phenomenon of change of the flow regime from turbulent to laminar is termed as "laminarization", "reverse transition", "inverse transition" or "relaminarization". However, this terminology is quite confusing, as it does not indicate whether the flow is accelerating or decelerating. Fernholz (1976) attempted to make some distinction between these two flows. According to him if the flow is initially turbulent and becomes laminar in a decelerated flow, it is termed relaminarization, and if it becomes laminar in an accelerated flow then it is called reverse transition.

Several acceleration parameters have been defined by various authors (Moretti and Kays, 1965, Patel and Head, 1968, Jones and Launder, 1972) to provide an indication of when an accelerated turbulent boundary layer flow would undergo a reverse transition process. The acceleration parameter defined by Moretti and Kays (1965) has been used to correlate the present problem. The acceleration parameter is expressed as follows:

$$K_v = \frac{v}{U_\infty^2}\frac{dU_\infty}{dr}, \tag{1}$$

where U_∞ is the free stream velocity which is approximated by the average velocity in the present case. Eq. (1) can be written as follows:

$$K_v = \frac{4G}{Re_{l2}}. \tag{2}$$

A turbulent flow would revert to laminar when $K_v \geqslant 3.5 \times 10^{-6}$ (Moretti and Kays, 1965).

The purpose of the present work is to study the velocity, turbulence intensity and pressure distributions for turbulent flow between two disks using both the experimental and the numerical techniques. The present work also examines the effect of acceleration on flow field.

2. Numerical model

2.1. Mean flow governing equations

The geometry and coordinate system used is shown in Fig. 1. The z and r origin is taken at the centre of the disk. The outer radius of the disk is assumed to be larger than the spacing between the disks. The elliptic flow regions at inlet and exit are assumed to be small and can be neglected. Therefore, the thin shear layer (Launder and Sharma, 1974) approximation is valid. The flow is steady, incompressible, viscous and axisymmetric. The approximate governing equations are as follows:

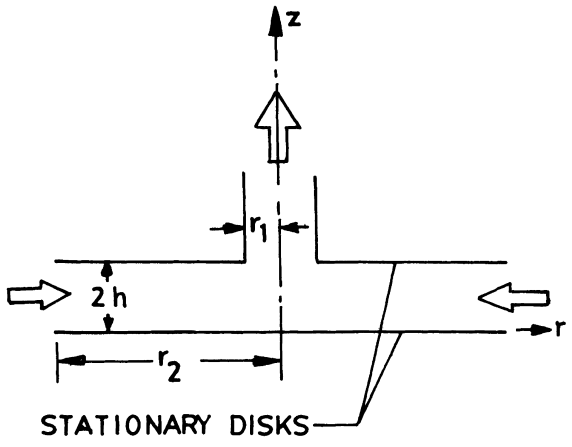

Fig. 1. Geometry and coordinate system.

Continuity equation

$$\frac{1}{r}\frac{\partial(ru)}{\partial r} + \frac{\partial w}{\partial z} = 0. \tag{3}$$

r-Momentum equation

$$u\frac{\partial u}{\partial r} + w\frac{\partial u}{\partial z} = -\frac{1}{\rho}\frac{dp}{dr} + v\frac{\partial^2 u}{\partial z^2} - \frac{\partial\overline{(u'w')}}{\partial z}, \tag{4}$$

where

$$-\overline{u'w'} = v_t\frac{\partial u}{\partial z}. \tag{5}$$

2.2. Turbulence model

The two equation (k–ε) turbulence model has been used to express v_t. According to this model the eddy viscosity can be expressed in terms of turbulence kinetic energy, k, and its dissipation rate, ε, as follows:

$$v_t = c_\mu\frac{k^2}{\varepsilon}, \tag{6}$$

k and ε are calculated from transport equations. These equations, under the thin shear layer approximation (Launder and Sharma, 1974), are as follows:

Turbulence kinetic energy

$$u\frac{\partial k}{\partial r} + w\frac{\partial k}{\partial z} = -\overline{u'w'}\frac{\partial u}{\partial z} + \frac{\partial}{\partial z}\left[\left(v + \frac{v_t}{\sigma_k}\right)\frac{\partial k}{\partial z}\right] - \varepsilon - 2v\left(\frac{\partial k^{1/2}}{\partial z}\right)^2. \tag{7}$$

Dissipation rate

$$u\frac{\partial \varepsilon}{\partial r} + w\frac{\partial \varepsilon}{\partial z} = -c_1\frac{\varepsilon}{k}\overline{u'w'}\frac{\partial u}{\partial z} + \frac{\partial}{\partial z}\left[\left(v + \frac{v_t}{\sigma_\varepsilon}\right)\frac{\partial \varepsilon}{\partial z}\right] - c_2\frac{\varepsilon}{k} + 2vv_t\left(\frac{\partial^2 u}{\partial z^2}\right)^2, \tag{8}$$

where the constants σ_k, σ_ε, c_1 are 1.0, 1.3, 1.44, respectively, for this type of flow. The parameters c_2 and c_μ are functions of turbulence Reynolds number, defined as $Re_t = k^2/v\varepsilon$ (Launder and Sharma, 1974):

$$c_\mu = 0.09\ \exp(-3.4/(1 + Re_t/50)^2). \tag{9}$$

$$c_2 = 1.92(1.0 - 0.3\ \exp(-Re_t^2)). \tag{10}$$

The corresponding boundary conditions are

$$u = w = k = \varepsilon = 0 \quad \text{at } z = 0,$$
$$\frac{\partial u}{\partial z} = w = \frac{\partial k}{\partial z} = \frac{\partial \varepsilon}{\partial z} = 0 \quad \text{at } z = h. \tag{11}$$

The pressure is estimated using the following integral continuity equation:

$$2\pi r \int_0^{2h} u \, dz = -Q. \tag{12}$$

2.3. Solution method

The coupled system of equations described by Eqs. (3)–(12) is a system of parabolic, partial non-linear differential equations and allows for a marching solution procedure. The control volume approach due to Patankar (1980) is utilized to discretise the governing equations. The calculation domain is divided into a number of non-overlapping control volumes surrounding each grid point. The differential equations are integrated over each control volume. On the basis of average value of the variables over a control volume, the finite difference forms of these equations are found. These equations are solved by the Gauss–Seidel (Blum, 1972) method. The solution is iterated till the residue to Eqs. (4), (7) and (8) is minimized below 10^{-5}, and the residue of Eq. (12) is minimized below 10^{-3}. The variables are under relaxed to get faster convergence. The relaxation parameter for radial velocity, turbulence kinetic energy and dissipation rate was 0.5. A relaxation factor of 0.9 was used for computation of pressure.

One of the most important aspects of k–ε models, is the specification of the turbulence intensities at the inlet. Turbulence intensities at the inlet were found to affect the entire flow field strongly. Therefore any arbitrary value at the inlet will result in misleading information. Hence a logical method developed by Shirazi and Truman (1988) for outward flow between two corotating disks, is utilized for the present model. The method is based on the philosophy that the inlet conditions must at least satisfy the approximate governing equations of turbulence kinetic energy and dissipation rate. Since the inlet conditions are approximate the finer grids were used in the inlet region to avoid numerical oscillations. The transport equations of k and ε are very stiff in the near wall region. At least eight to ten grids must be accommodated in the viscous sublayer region. For this purpose the variable grid spacing of Cebeci et al. (1970) is employed in z-direction as well as in r-direction. The grid dependency of the solution is tested by successively refining the mesh. The solution is treated as grid independent when further refinements of a mesh does not change the pressure by more than 10^{-3}. Typically, 80 grids in z-direction is sufficient. The increment in grid spacing was 5–12% to allow finer mesh near the wall. The grid spacing in the radial direction was 10^{-3} near the inlet and was 10^{-2} away from the inlet.

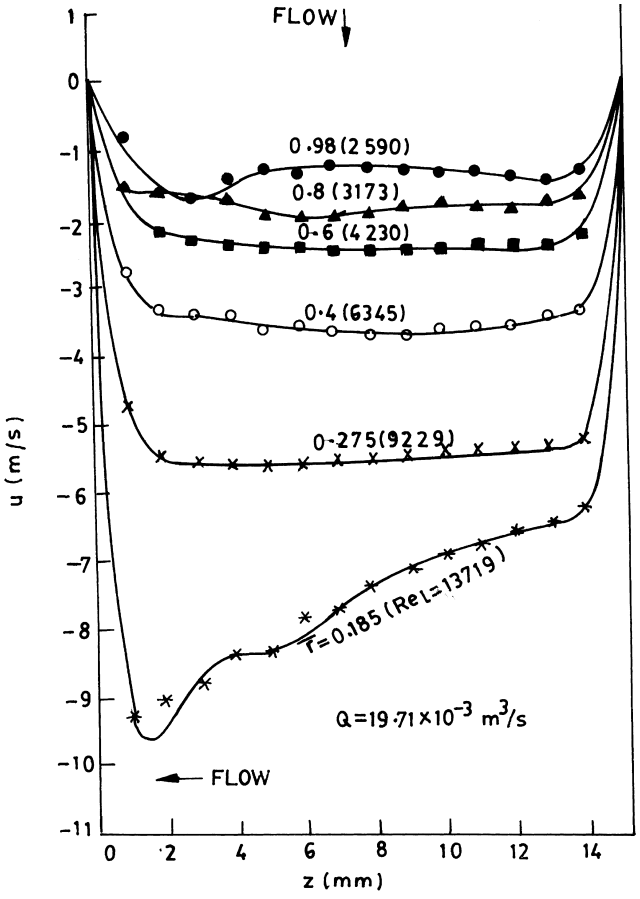

Fig. 3. Radial velocity distribution at different radial locations (experimental). $d_2/d_1 = 6$, $G = 0.05$, $Re_{l2} = 2538$.

3. Experiment

3.1. Experimental set-up

A schematic diagram of the experimental set-up is shown in Fig. 2. The experimental set-up was specially designed to study

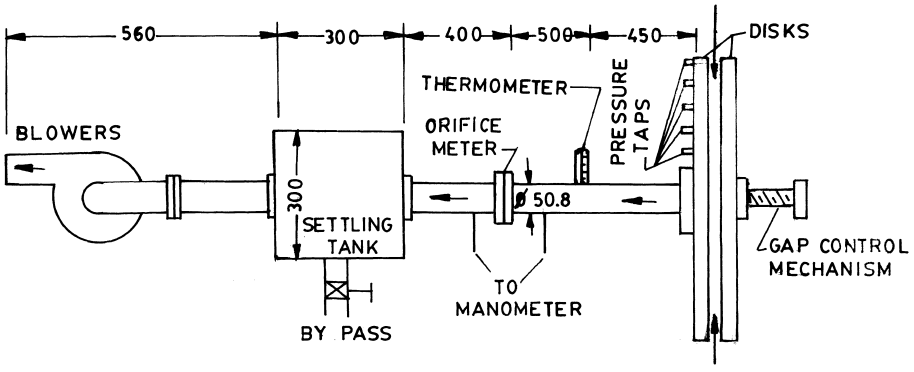

Fig. 2. Schematic of experimental set-up.

this problem and consisted of two parallel disks of diameter 302.4 mm. The disks' edges were rounded according to the recommendations of Beavers et al. (1970) to induce separation free entry of air at the peripheral gap of the disks. One disk with a concentric hole was connected to a suction blower. Another disk was mounted on a threaded spindle, which could move to and for in a sleeve to enable one to change the gap between the disks. The air flow was measured by a calibrated orifice meter provided in the suction pipe. A settling tank was provided in the circuit to reduce disturbances.

3.2. Instrumentation

A DANTEC two color beam (green and blue) LDA system in back scatter mode using an argon ion laser was used for measurement of the velocity and velocity and turbulence intensity. The optical probe was mounted on a traverse mechanism, which allowed the movement of the probe in three perpendicular directions. A blast type seed generator using dioctyl phthalate was used to generate seed particles. Seeds were introduced in the air away from the inlet so that they could attain the velocity of the air prior to reaching the peripheral gap between the disks. The probe was adjusted in such a way that the laser beams intersected at the point where the measurement has to be taken. The plane of the beams is kept parallel to the disk surface and the axis of the probe lens was perpendicular to the direction of the flow. The seed particles passing through the interference fringes scattered light which was then received by the probe. The optical signals were sent to a Burst Spectrum Analyzer where the optical signals were converted into velocity components. The measurements were taken in the z-direction at various radial locations by changing the probe positions. Pressure measurements were carried out with manometers connected to pressure taps provided at different radial locations.

Uncertainty in the measured quantities was due to the inaccuracy in experimental set-up and to the limitations of the measuring instruments. The procedure of Kline and McClintock (1953) was followed for estimation of uncertainty. Uncertainties in gap, radial position and probe position were estimated to be 0.5%. Uncertainty in non-dimensional pressure is 5%. Uncertainty in Reynolds number is 4%. The uncertainty in velocity and turbulence intensity could not be established exactly, however, a rough estimate of uncertainty in these quantities was below 3%.

4. Results and discussions

4.1. Radial velocity profile

Figs. 3 and 4 show the plots of radial velocity versus axial direction z (where z is measured from the disk having discharge hole). It is evident from the figures that the average velocity increases in the direction of flow (magnitude) due to decrease in the cross sectional area of flow. It may be observed that the

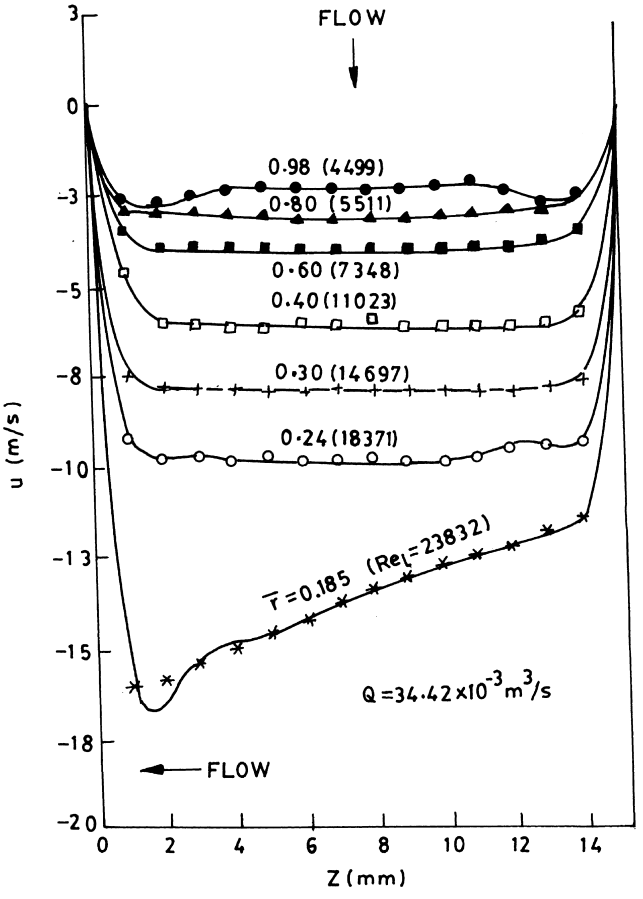

Fig. 4. Radial velocity distribution at different radial locations (experimental). $d_2/d_1 = 6$, $G = 0.05$, $Re_{l2} = 4409$.

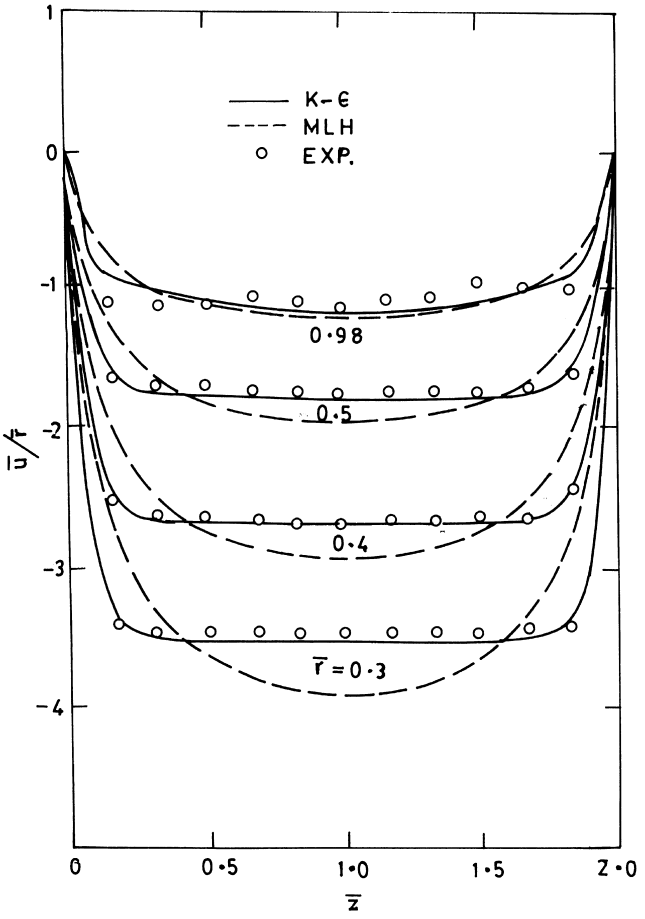

Fig. 5. Comparison of radial velocity distribution obtained by theoretical model [MLH and k–ε] with experimental data (LDA). $Re_{l2} = 2538$, $G = 0.0394$.

velocity profile at the inlet shows some entry effect due to the fluid entering from the infinite medium. However, the velocity profile is symmetrical about mid plane, i.e., $z=h$ (where $2h$ is the gap between two disks). The velocity profiles at $\bar{r}=0.8$–0.24 are symmetrical about the mid plane. However the velocity profile at $\bar{r}=0.185$ is not symmetrical and shows a maximum velocity near the disk with the central hole (sink). The asymmetry is due to the fact that the sink is located only in one of the disks. The asymmetry is close to the sink hole.

Closed form expressions of radial velocity profile and pressure distribution for turbulent source flow between two disks have been derived by Singh et al. (1994). The expressions are obtained using the mixing length hypothesis (MLH). These expressions are modified for the present situation and used for comparison purposes. The radial velocity profile from the numerical model was compared with both the LDA measurements and the MLH.

It can be seen from Fig. 5 that the numerical predictions are in good agreement with experimental data. This means that the numerical model is suitable for studying the present flow. It can be also observed from the figure that the predictions of the k–ε model are more accurate than that of MLH.

The radial velocities obtained by numerical model were also compared with the universal logarithmic profile (Tabatabai and Pollard, 1987). The velocity distribution normalized by friction velocity in viscous sublayer is

$$u^+ = z^+ \tag{13}$$

and the logarithmic distribution is

$$u^+ = A\log_{10}z^+ + B. \tag{14}$$

The values of A and B are taken as zero pressure gradient values ($A=5.5$ and $B=4.45$). Fig. 6 shows the velocity obtained from the numerical model along with the values obtained from Eqs. (13) and (14), respectively. It is evident from these figures that the numerical predictions are closer to the velocity distribution in viscous sublayer. However there is some discrepancy in the logarithmic distribution region because the equation represents the constant pressure gradient flow.

4.2. Turbulence kinetic energy

The distributions of the relative turbulence intensity in the radial direction, $((u'^z)^{1/2}/U)\times 100$ is plotted in Fig. 7 (Singh, 1993). The curves in this figure show that the turbulence intensity is maximum near the disks and more or less constant in the core region. This is due to the fact that the maximum production of the turbulence kinetic energy occurs in the transition layer (between viscous sublayer and turbulence region) of a turbulent boundary layer and away from the wall it decreases. Laufer and Clark's (Chien, 1982) data for pipe flow show that the turbulence kinetic energy (hence turbulence fluctuations) increases with Reynolds number. Unlike pipe flow, in the present flow situation, the fluctuations are decreasing with the increase in Reynolds number. The reason for

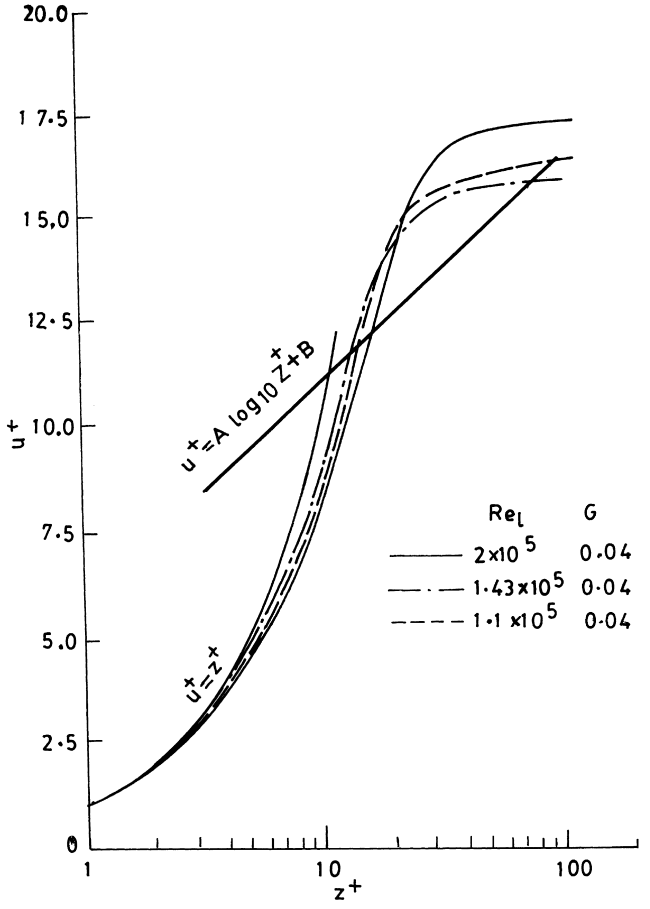

Fig. 6. Comparison of radial velocity distribution obtained by numerical model [k–ε] with classical viscous sublayer and logarithmic profiles.

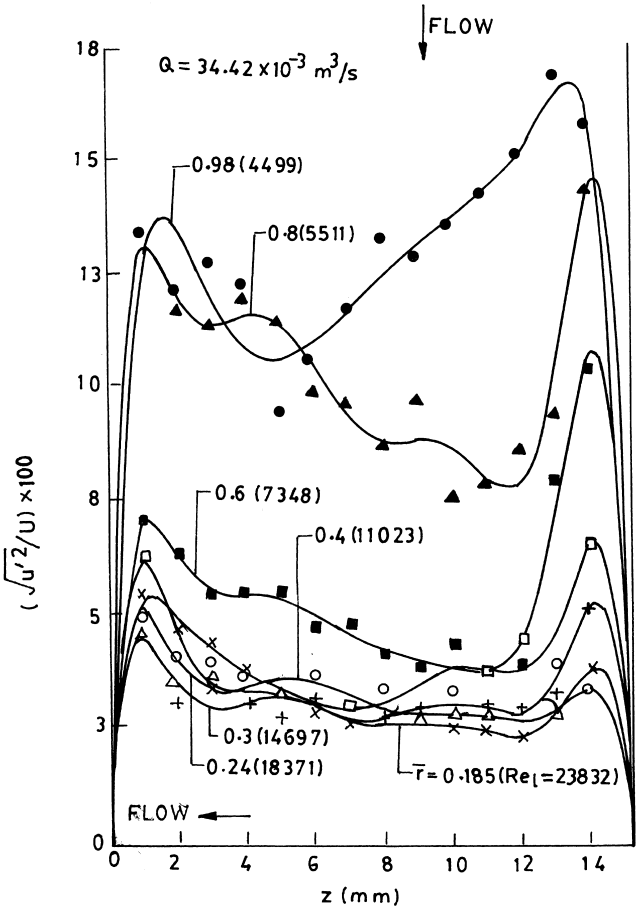

Fig. 7. Relative turbulence intensity distribution at different radial locations [experimental]. $d_2/d_2=6$, $G=0.05$, $\mathrm{Re}_{l2}=4409$.

this is the adverse effect of acceleration on the production of turbulence kinetic energy, which suppresses the turbulence fluctuations.

The turbulence kinetic energy distribution obtained from the numerical model for gap ratios of 0.01, 0.02, 0.05 ($K_v = 0.8 \times 10^{-6}$, 1.6×10^{-6}, 4×10^{-6}) is shown in Fig. 8. As gap ratio decreases the location of maximum kinetic energy moves away from the wall and its magnitude decreases. This behavior indicates a gradual increase in the viscosity dominated region and a decrease in the energy production in the viscous sublayer. It means the decrease in gap ratio has a stabilizing effect on the flow. For the same inlet conditions, the turbulence kinetic energy decay faster at low gap ratio despite the fact that the acceleration parameter is low for the low gap ratio. This shows that, in addition to acceleration parameter, gap ration is also an important parameter for this flow situation.

4.3. Friction factor

The friction factor, calculated with the help of velocity gradient at disk surface, has been plotted in Fig. 9 showing the effect of inlet local Reynolds number. The friction factor increases up to $\bar{r} \cong 0.88$ but drops further downstream. The friction factor increases with a decrease in radius for $\bar{r} \leqslant 0.88$. The curves up to $Re_{l2} = 10^5$ are of S shape which resemble the well-known friction factor distribution for pipe flow with a sudden increase in friction factor in a transition region. The friction factor increases as Re_l increases in flow direction due to reverse transition. The reverse transition up to inlet local

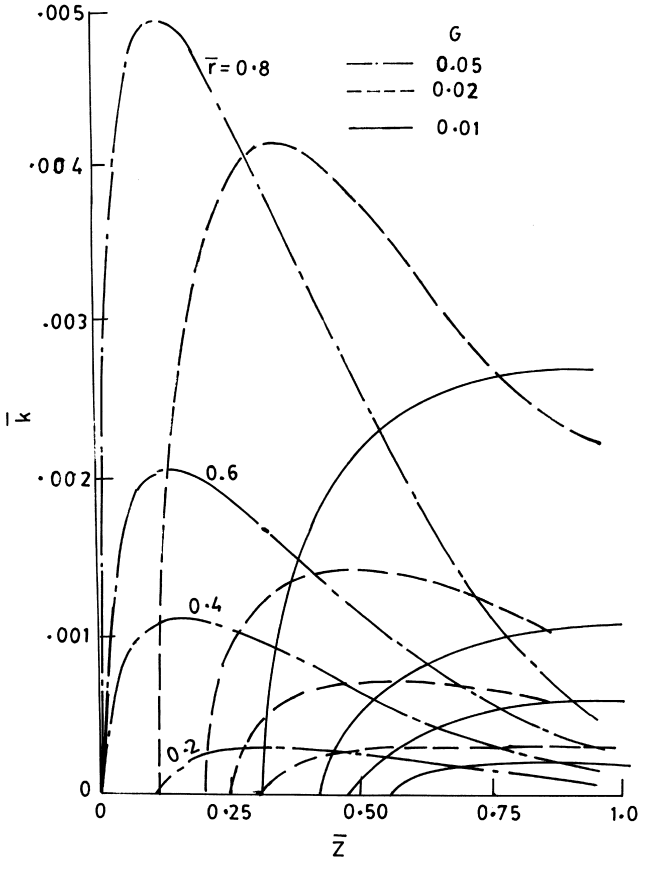

Fig. 8. Turbulence kinetic energy distribution [k–ε] for different gap ratios. $Re_{l2} = 5 \times 10^4$.

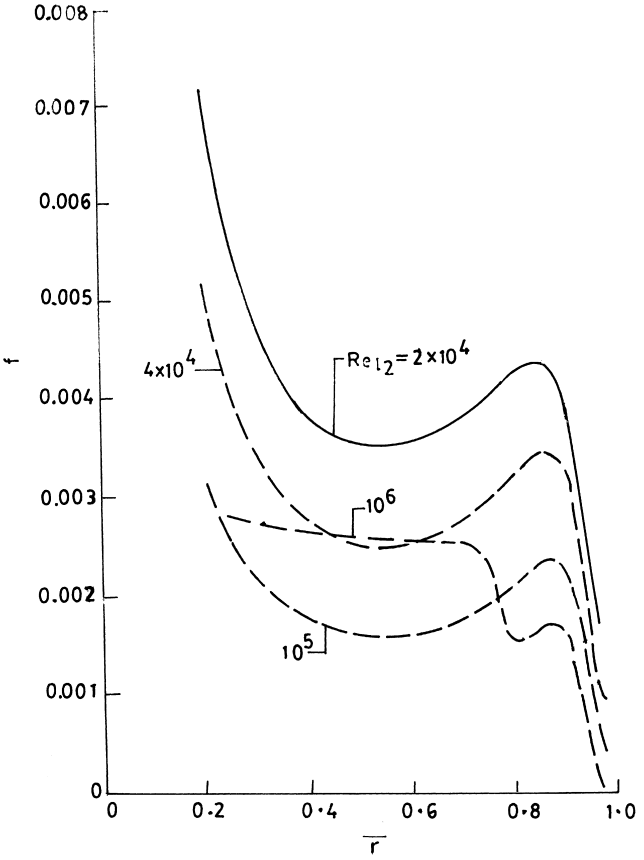

Fig. 9. Friction factor distribution [k–ε] for different inlet local Reynolds number. $G = 0.04$.

Reynolds number 4×10^4 is expected since the acceleration parameter is higher than 3.5×10^{-6}. The reverse transition is taking place even at a low acceleration parameter, i.e. 1.6×10^{-6} ($Re_{l2} = 10^5$) in the present flow situation. But at the very low acceleration parameter of 1.6×10^{-7} ($Re_{l2} = 10^6$) the flow, after undergoing reverse-transition process, reverts to the turbulence regime showing a nearly constant friction factor further down stream. The results could not be obtained for an acceleration parameter lower than 1.6×10^{-7} due to convergence problem.

4.4. Pressure distribution

The static pressure distribution is plotted in Fig. 10. The pressure decreases with radius, partly due the viscous and turbulent losses and partly due to inertial contribution. Since inertial contribution is proportional to $1/r^3$, pressure decreases rapidly at lower radius. It is evident from figure that the k–ε model predicts pressure distribution close to experimental data.

5. Conclusion

The velocity and pressure predicted using the k–ε model are close to experimental data. The flow undergoes a reverse-transition when the acceleration parameter is 1.6×10^{-6}, which is much lower than the value reported in the open literature for other accelerating flows. The acceleration parameter decreases with gap ratio for a fixed Reynolds number. Turbulence level should be higher for a low acceleration parameter. Contrary to

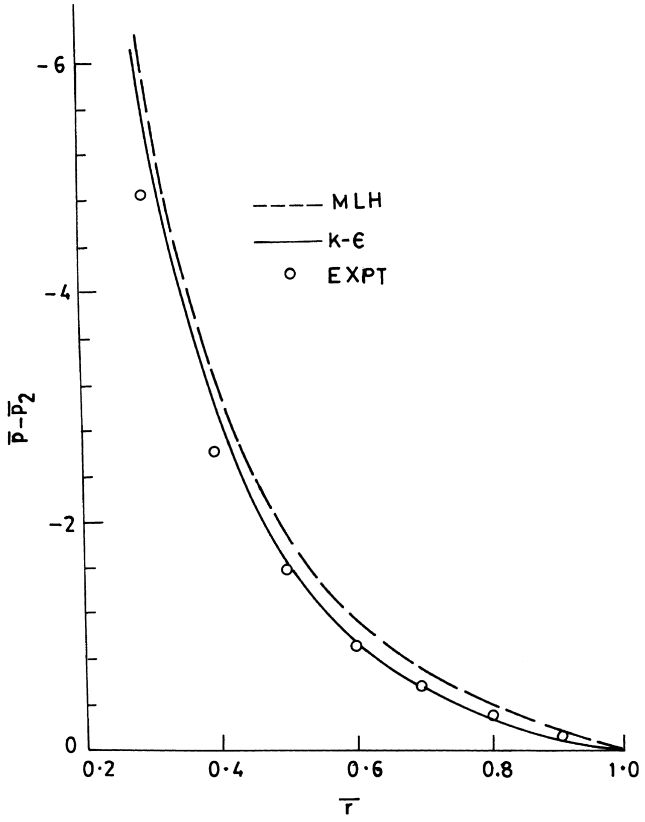

Fig. 10. Comparison of pressure distribution obtained by theoretical models [MLH and k–ε] with experimental data. $Re_{12} = 5748$, $G = 0.0197$.

this the turbulence kinetic energy decays faster at lower gap ratios for a fixed Reynolds number. This shows that the acceleration parameter as well as gap ratio play important roles. Further investigation is required to establish the criteria for the on-set of reverse transition.

References

Beavers, G.S., Sparrow, E.M., Magnuson, R.A., 1970. Experiments on hydro-dynamically developing flow in rectangular ducts of arbitrary aspects ratio. Int. J. Heat Mass Transfer 13, 689–694.

Blum, E.K., 1972. Numerical Analysis and Computational Theory and Practice, Addison–Wesley, California, pp. 135–143.

Cebeci, T., Smith, A.M.O., Mosinskis, G., 1970. Solution of the incompressible turbulent boundary layer equation with heat transfer. ASME Trans. J. Heat Transfer 102, 133–143.

Chien, K.Y., 1982. Prediction of channel and boundary layer flows with low Reynolds number turbulence model. AIAA J. 20, 33–38.

Ervin, J.S., Suryanarayana, N.V., Ng, H.C., 1989. Radial turbulent flow of a fluid between two coaxial disks. Trans. ASME J. Fluids Engg. 111, 378–383.

Fernholz, H.H. 1976. External flows. In: Bradshaw, P.(Ed.), Topics in Applied Physics: Turbulence. Springer, Berlin, pp. 45–98.

Garcia, C.E., 1969–1970. Unsteady air flow between two disks at low velocity. Proc. Instn. Mech. Engrs. 184, 913–923.

Jones, W.P., Launder, B.E., 1972. Prediction of relaminarization with a two equation model of turbulence. Int. J. Heat Mass Transfer 15, 301–314.

Kline, S.J., McClintock, F.A., 1953. Describing uncertainties in single sample experiments. Mech. Engg. 75, 3–8.

Kreith, F., 1965. Reverse transition in radial source flow between two parallel planes. Phys. Fluids 8, 189–193.

Launder, B.E., 1964. Laminarization of the turbulent boundary layer in a severe acceleration. Trans. ASME J. Appl. Mech. 31, 707–708.

Launder, B.E., Sharma, B.I., 1974. Application of energy dissipation model of turbulence to the calculation flow near a spinning disk. Lett. Heat Mass Transfer 1, 131–138.

Lee, P.M., Lin, S., 1985. Pressure distribution for radial inflow between narrowly spaced disks. Trans. ASME J. Fluids Engg. 107, 338–341.

McGinn, J.H., 1956. Observations of the radial flow of water between fixed parallel plates. Appl. Sci. Res. 5, 255–264.

Moller, P.S., 1963. Radial flow without swirl between parallel disks. Aeronaut. Quart. 14, 163–186.

Moretti, P.M., Kays, W.M., 1965. Heat transfer to a turbulent boundary layer with varying free stream velocity and varying surface temperature: An experimental study. Int. J. Heat Mass Transfer 8, 1187–1202.

Murphy, H.D., Coxon, M., McEligot, D.M., 1978. Symmetric sink flow between parallel plates. Trans. ASME J. Fluids Engg. 100, 477–484.

Murphy, H.D., Chambers, F.W., McEligot, D.M., 1983. Converging flow. Part 1. Mean flow. J. Fluid Mech. 127, 379–401.

Patankar, S.V. 1980. Numerical Heat Transfer and Fluid Flow. Hemisphere Publishing, Washington, DC.

Patel, V.C., Head, M.R., 1968. Reversion fo turbulent to laminar flow. J. Fluid Mech. 34, 371–392.

Shirazi, S.A., Truman, C.R., 1988. Prediction of turbulent source flow between corotating disks with an anisotropic two equation turbulence model. Trans. ASME J. Turbomachinery 111, 187–194.

Singh, A., Vyas, B.D., Powle, U.S., 1994. Turbulent Source Flow between Two Disks. Proceedings of 21st NCFMFP, Hyderabad, India.

Singh, A., 1993. Theoretical and experimental investigations on inward flow between two disks. Ph.D. Thesis, IIT Bombay, India.

Tabatabai, M., Pollard, A., 1987. Turbulence in radial flow between parallel disks at medium and low Reynolds number. J. Fluid Mech. 185, 483–502.

Vatistas, G.H., 1988. Radial flow between two closely placed disks. AIAA J. 26, 887–890.

Vatistas, G.H., 1990. Radial inflow within two flat disks. AIAA J. 28, 1308–1311.